The influence of current meteorological phenomena on flight processes

Gabriela-Liliana STROE[1,2], Renata SEPTICHITA*[,2], Valentin SOARE[2], Adrian BURGHIU[2]

*Corresponding author
[1]Faculty of Aerospace Engineering,
National University of Science and Technology POLITEHNICA Bucharest,
Splaiul Independentei 313, 060042, Bucharest, Romania
[2]INCAS – National Institute for Aerospace Research "Elie Carafoli",
B-dul Iuliu Maniu 220, Bucharest 061126, Romania,
stroe.gabriela@incas.ro, septichita.renata@incas.ro*, soare.valentin@incas.ro,
burghiu.adrian@incas.ro

DOI: 10.13111/2066-8201.2026.18.1.9

Received: 18 December 2025/ Accepted: 21 February 2026/ Published: March 2026

Abstract: *This paper presents atmospheric turbulence as an intrinsic hazard to aircraft flight dynamics, particularly when flying over large oceanic expanses bodies of water such as the Pacific Ocean. This study applies the von Kármán atmospheric turbulence model to the lateral, longitudinal, and vertical perturbations experienced by a medium-range twin-engine passenger aircraft. Mathematical expressions for the turbulence inputs are derived and integrated into the linearised aircraft equations of motion, and the dynamic response under cruise flight conditions is analysed. The results reveal key insights into turbulence structure and demonstrate the utility of stochastic filtering for state estimation in high-noise environments.*

Key Words: *atmospheric turbulence, numerical simulation, wind fluctuation statistics*

1. INTRODUCTION

Convective atmospheric turbulence presents critical challenges to aircraft performance and safety, especially over vast oceanic regions such as the Pacific Ocean. In this study, atmospheric turbulence is modelled using the von Kármán spectrum, its impacts on aircraft dynamics are simulated, and an Extended Kalman Filter is applied to estimate turbulent states and aircraft state vectors in real time [8-10].

Turbulence in convective weather arises from buoyancy-driven vertical motions, wind shear, and thermal plumes.

Over oceans, the absence of terrain does not preclude the formation of large-scale turbulent structures, which are often driven by sea surface temperature gradients.

These turbulent motions can degrade passenger comfort, impact aircraft stability, and complicate flight control demands. To characterize this phenomenon, a stochastic turbulence model based on the von Kármán spectrum, widely used in atmospheric science and aerospace engineering is adopted [13-14].

2. STATE OF THE ART IN METEOROLOGICAL PHENOMENA AFFECTING AIRCRAFT OPERATIONS

Atmospheric turbulence directly affects aircraft stability, passenger comfort, structural loads, and flight control system performance. Over the Pacific Ocean, turbulence sources include jet streams, convective cells, and gravity wave activity. Among turbulence models, the von Kármán spectral model captures realistic wind fluctuation statistics across a wide range of scales, suitable for high-fidelity simulation [11-12].

In aerospace dynamics, turbulence is treated as a stochastic disturbance with a defined Power Spectral Density (PSD). The von Kármán PSD expression includes the following terms for longitudinal (u), lateral (v), and vertical (w) gusts [15-17].

In this article, we examine:

- The influence of convective meteorological phenomena on a civil aircraft at various flight levels and speeds.
- The application of the von Kármán turbulence model in MATLAB to simulate gusts and turbulent environments.
- The assessment of aircraft response (including acceleration, loads, control demands) across different flight regimes over the Pacific Ocean.

The dynamics of aviation turbulence are described in several recent review studies. As an example, "Aviation Turbulence: Dynamics, Forecasting, and Response to Climate Change" reviews the role of vertical shear instabilities, convective processes, and mountain waves in generating atmospheric turbulence [18-19].

Convective phenomena – including thermals, cumulonimbus clouds, and towering cumulus – over oceanic regions can also generate turbulence, even under clear-air conditions, through mechanism such as gravity waves, and wind shear. While many studies focus on turbulence within atmospheric boundary layers, others investigate free-stream turbulence affecting aircraft during oceanic flights [18-19].

For example, the Activate programme observed turbulence in both cloud-topped and cloud-free boundary layers over the Atlantic Ocean. Although the Pacific Ocean exhibits different characteristics – such as thermal structures, jet-streams, convective zones, and tropical and equatorial dynamics – the general turbulence modelling approaches remain applicable [15-17].

One important caveat is that many existing studies focus on low-altitude turbulence within the atmospheric boundary layer or near ground-based obstacles. At high-altitude cruise conditions (FL300 and above) over oceanic regions, the turbulence environment is markedly different, being dominated by clear-air turbulence and shear layers.

Consequently, turbulence model parameters – such as scale length and intensity – must be appropriately adapted [8-10].

Several simulation-based studies have applied stochastic turbulence models, including the von Kármán spectrum, to aircraft flight analysis. For example, "Simulation of aircraft flights with turbulence and icing conditions", uses a von Kármán spectrum to simulate turbulence for flight simulation.

Another study, "Estimation of Aircraft – Dependent Bumpiness Severity in Turbulent Flight", uses the von Kármán model to generate time series and compute vertical acceleration severity. However, explicit empirical studies of civil aircraft over the Pacific Ocean under convective turbulence with full flight level/airspeed variation remain limited [5-7].

The present study fills this gap by combining computational modelling, simulation, and targeted flight scenarios.

Table 1 – The representative airspeeds used in this study

Flight Level	Speed (m/s)	Turbulence Regime	σ_w (m/s)	L_w (m)
FL300	230	Mild	0.5	60
FL300	250	Moderate	1.0	100
FL300	270	Strong	2.0	150
FL350	230	Mild	0.5	60
…	…	…	…	…
FL390	270	Strong	2.0	150

Over the Pacific Ocean, convective zones – e.g., near the ITCZ, tropical convection – or mid-latitudes can generate turbulence at these altitudes [5-7]. Accordingly, this study considers a set of representative airspeeds (230 m/s, 250 m/s, and 270 m/s) and several flight levels (FL300, FL350, and FL390).

At higher airspeed – e.g. 270 m/s – the effective temporal frequency of gust encounters is higher, because the aircraft samples shorter spatial scales faster, so for fixed scale length the amplitude of vertical acceleration may be higher [5-7].

At a higher flight level – FL390 – turbulence intensity may be lower – depending on the convective or clear-air environment. However, the proximity of shear and jet streams may offset this, resulting in non-linear behaviour [5-7].

In strong turbulence regimes, the aircraft may experience vertical acceleration peaks beyond typical comfort thresholds – e.g. >1.5 g – even though mean load remains near 1.0 g [5-7].

Sensitivity of results to turbulence scale length: larger yields slower varying gusts – longer wavelength – which may excite aircraft modes differently than short-scale gusts [5-7].

The Lorenz energy cycle represents atmospheric energy in terms of zonal-mean and eddy kinetic energy as well as available potential energy, corresponding to large-scale, small-scale, and potential energy components, respectively [1-2]:

$$\bar{K}_L \equiv \left\langle \rho_0 \frac{\bar{u}^2}{2} \right\rangle \tag{1}$$

$$K'_L \equiv \left\langle \rho_0 \frac{\overline{u'^2} + \overline{v'^2}}{2} \right\rangle \tag{2}$$

$$\bar{P}_L \equiv \frac{1}{2} \left\langle \frac{\rho_0}{N^2} \left(\frac{\partial \bar{\Phi}}{\partial z} \right)^2 \right\rangle \tag{3}$$

$$P'_L \equiv \frac{1}{2} \left\langle \frac{\rho_0}{N^2} \overline{\left(\frac{\partial \Phi'}{\partial z} \right)^2} \right\rangle \tag{4}$$

The energy transformations [2]:

$$[\overline{P_L} \cdot \overline{K_L}] \equiv \left\langle \rho_0 \overline{w} \frac{\partial \bar{\Phi}}{\partial z} \right\rangle \tag{5}$$

$$[P'_L \cdot K'_L] \equiv \left\langle \rho_0 w' \frac{\partial \Phi'}{\partial z} \right\rangle \tag{6}$$

$$[K'_L \cdot \bar{K}_L] \equiv \left\langle \rho_0 \overline{u'v'} \frac{\partial \bar{u}}{\partial y} \right\rangle \tag{7}$$

$$[P'_L \cdot \overline{P_L}] \equiv \left\langle \frac{\rho_0}{N^2} v' \frac{\overline{\partial \Phi'}}{\partial z} \frac{\partial^2 \bar{\Phi}}{\partial y \, \partial z} \right\rangle \tag{8}$$

Also, the source [1-2]:

$$\bar{R}_L \equiv \left\langle \frac{\rho_0}{N^2} \frac{\kappa \bar{J}}{H} \frac{\partial \bar{\Phi}}{\partial z} \right\rangle \tag{9}$$

$$R'_L \equiv \left\langle \frac{\rho_0}{N^2} \frac{\overline{\kappa J'}}{H} \frac{\overline{\partial \Phi'}}{\partial z} \right\rangle \tag{10}$$

$$\bar{\varepsilon}_L \equiv \langle \rho_0 \bar{u} \bar{X} \rangle \tag{11}$$

$$\varepsilon'_L \equiv \langle \rho_0 (\overline{u'X'} + \overline{v'Y'}) \rangle \tag{12}$$

Integrating over the volume [3-4]:

$$\frac{d}{dt} \langle \frac{\rho_0 \bar{u}^2}{2} \rangle = + \langle \rho_o \bar{\Phi} \frac{\partial \bar{v}}{\partial \mathrm{y}} \rangle + \langle \rho_o \overline{u'v'} \rangle + \langle \rho_0 \bar{u} \bar{X} \rangle \tag{13}$$

$$\frac{d}{dt} \langle \frac{\rho_0}{2N^2} \left(\frac{\partial \bar{\Phi}}{\partial \mathrm{z}} \right)^2 \rangle = - \langle \rho_0 \bar{w} \frac{\partial \bar{\Phi}}{\partial \mathrm{z}} \rangle + \langle \frac{\rho_0 k \bar{J}}{N^2 H} \left(\frac{\partial \bar{\Phi}}{\partial \mathrm{Z}} \right) \rangle - \langle \frac{\rho_0}{N^2} \frac{\partial \bar{\Phi}}{\partial \mathrm{Z}} \frac{\partial}{\partial \mathrm{Y}} \left(\overline{v' \frac{\partial \Phi'}{\partial \mathrm{z}}} \right) \rangle \tag{14}$$

$$\frac{d}{dt} \langle \rho_0 \frac{\overline{u'^2} + \overline{v'^2}}{2} \rangle = + \langle \rho_0 \overline{\Phi' \left(\frac{\partial \Phi'}{\partial \mathrm{x}} + \frac{\partial v'}{\partial \mathrm{y}} \right)} \rangle - \langle \rho_0 \overline{u'v'} \frac{\partial \bar{u}}{\partial \mathrm{y}} \rangle + \langle \rho_0 (\overline{u'X'} + \overline{v'Y'}) \rangle \tag{15}$$

$$\frac{d}{dt} \langle \frac{\rho_0}{2N^2} \overline{\left(\frac{\partial \Phi'}{\partial \mathrm{z}} \right)^2} \rangle = - \langle \rho_0 w' \frac{\overline{\partial \Phi'}}{\partial \mathrm{z}} \rangle + \langle \frac{\overline{\rho_0 k J' \frac{\partial \Phi'}{\partial \mathrm{z}}}}{N^2 H} \rangle - \langle \frac{\rho_0}{N^2} \left(\frac{\partial^2 \bar{\Phi}}{\partial \mathrm{z} \, \partial \mathrm{y}} \right) \left(\overline{v' \frac{\partial \Phi'}{\partial \mathrm{z}}} \right) \rangle \tag{16}$$

Equations (3), (13), (14), (15), and (16) can therefore be reformulated in a simplified form [1-2]:

$$\frac{d\bar{K}_L}{dt} = [\bar{P} \cdot \bar{K}] + [K' \cdot \bar{K}] + \bar{\varepsilon} \tag{17}$$

$$d\bar{P}_L/dt = -[\bar{P} \cdot \bar{K}] + [P' \cdot \bar{P}] + \bar{R} \tag{18}$$

$$dK'_L/dt = [P' \cdot K'] - [K' \cdot \bar{K}] + \varepsilon' \tag{19}$$

$$dP'_L/dt = -[P' \cdot K'] - [P' \cdot \bar{P}] + R' \tag{20}$$

Rate of change of total energy [1-2]:

$$d(\bar{K}_L + K'_L + \bar{P}_L + P'_L)/dt = \bar{R}_L + R'_L + \bar{\varepsilon} + \varepsilon' \tag{21}$$

This equilibrium is critical for ensuring stability and regulating the general dynamics of the atmospheric system:

$$\bar{R}_L + R'_L = -\bar{\varepsilon} - \varepsilon' \tag{22}$$

Can be expressed as [3-4]:

$$\frac{D}{Dt}(q_v) = P_v \tag{23}$$

where:

q_v – the water vapour mixing ratio;

P_v – the sum of all sources and sinks;

$\rho_s(x, y, t)$ – the evolution of the surface pressure.

The transformed continuity equation [3-4] is given in:

$$\frac{\partial \rho_0}{\partial t} + \bar{V} \cdot (\rho_0 V) + \rho_s \frac{\partial \dot{\sigma}}{\partial \sigma} = 0 \tag{24}$$

Integrating (24) vertically and using $\dot{\sigma} = 0$ and $\sigma = 0$ we obtain the result [3-4]:

$$\frac{\partial p_S}{\partial t} = -\int_0^1 \nabla \cdot (p_S V) d\sigma \tag{25}$$

At leading order, the Taylor series can be approximated by [3-4]:

$$T(R_0 + \delta R) = T(R_0) + \frac{\partial T}{\partial R}\Big|_{R_0} \delta R \tag{26}$$

T – temperature; R – parameter; R_0 – value for the unperturbed climate.

The magnitude of this perturbation determines the system's response in a directly proportional manner [3-4]:

$$\partial T_L = \frac{\partial T}{\partial R}\Big|_{R_0} \delta R = \lambda \delta R \tag{27}$$

λ – climate sensitivity parameter.

$$\delta T_L = \delta T_0 + f \delta T \tag{28}$$

where f, the feedback factor, governs the amplification [3-4].

α_i – physical process

$$\delta T_L = \lambda \delta R_0 + \lambda \sum_i \frac{\partial R}{\partial \alpha_i} \frac{\partial \alpha_i}{\partial T} \partial T \tag{29}$$

In order to establish the equivalence between the prior result and equation (28), it is necessary to define the feedback factor [3-4]:

$$f_L = \lambda \sum_i \frac{\partial R}{\partial \alpha_i} \frac{\partial \alpha_i}{\partial T} \tag{30}$$

Equation (28) can be solved for δT [3-4]:

$$\delta T_L = \frac{\delta T_0}{1 - f} \tag{31}$$

The model represents the sea surface temperature anomaly in the eastern Pacific, T, using the following governing equation [3-4]:

$$\frac{dT_L}{dt} = bT(t) - cT(t-\tau) \tag{32}$$

b, c – positive constants; τ – time delay.

The study explores the relationships and mechanisms governing synoptic-scale tropical motions and their interactions with convective activity [3-4].

$$\left(\frac{\partial}{\partial_t} + V\cdot\nabla + {w^*}_L\frac{\partial}{\partial z^*}\right)V + fk\times V = -\nabla\Phi \tag{33}$$

$$\partial\Phi/\partial {z^*}_L = RT/H \tag{34}$$

$$\partial u/\partial x + \partial v/\partial y + \partial {w^*}_L/\partial {z^*}_L - {w^*}_L/H = 0 \tag{35}$$

$$\left(\frac{\partial}{\partial t} + V\cdot\nabla\right)T + {w^*}_L N^2 H/R = \frac{J}{c_p} \tag{36}$$

$$\partial u/\partial x + \partial v/\partial y \le U/L \tag{37}$$

For length scales comparable to the density scale height H, the analysis becomes [3-4]:

$$\partial {w^*}_L/\partial z^* - {w^*}_L/H \sim W/H \tag{38}$$

Forces that dominate and regulate atmospheric motion across different scales [3-4]:

$$(V\cdot\nabla)V \sim U^2/L \tag{39}$$

$$|\partial V/\partial t|/|(V\cdot\nabla)\mathrm{V}| \sim 1 \tag{40}$$

$$|{w^*}_L\partial V/\partial {z^*}_L|/|(V\cdot\nabla)\mathrm{V}| \sim WL/UH \le 1 \tag{41}$$

$$|fk\times V|/|(V\cdot\nabla)\mathrm{V}| \sim fL/U = R_0^{-1} \le 1 \tag{42}$$

$$|\nabla\Phi|/|(V\cdot\nabla)\mathrm{V}| \sim \delta\Phi/U^2 \tag{43}$$

$$ {w^*}_L(N^2H/R) = J/c_p \tag{44}$$

J – the radiative flux; c_p – the specific heat capacity at constant pressure.

For the tropical troposphere [1-4]:

$$N^2K/R \sim 3Kkm^{-1} \tag{45}$$

Vertical motion scale satisfies the following relations [3-4]:

$$W \sim 0.3\ cm\ s^{-1} \tag{46}$$

$$WL/UH \sim 0.03 \tag{47}$$

3. THEORETICAL FRAMEWORK, NUMERICAL SIMULATIONS AND CONCLUSIONS

We interpret results in the context of aircraft operations over the Pacific Ocean. Key observations include:

- Over oceanic convective zones, upward motion and turbulence may be stronger at lower altitudes, but at cruise altitudes, residual convection and jet-stream induced clear-air

turbulence dominate. The von Kármán model is a generic representation; actual turbulence associated with convective phenomena may deviate from there assumptions, being non-stationary, anisotropic, and intermittent.

- The von Kármán model assumes stationary, isotropic turbulence, whereas convective turbulence may contain coherent structures (plumes, thermals) that violate these assumptions. Therefore, the simulation results should be interpreted with caution.
- The simulation illustrates how speed and altitude interact with turbulence scale length and intensity to influence aircraft responses. For route planning, flying at lower speed – within the safe operational envelope – may reduce gust encounter frequency and potentially lower peak loads.

This study investigates the response of a commercial airliner cruising at high altitude over the Pacific Ocean through a region of intense convective activity, which results in strong turbulence. A stochastic gust field is generated using the von Kármán spectral model for continuous gusts. The aircraft dynamics are simulated in MATLAB to evaluate acceleration, load factor, structural bending moments, and trajectory perturbations. Key results include time series of gust wind components, power spectral densities, aircraft responses – including vertical acceleration and roll/pitch rates – and statistical metrics of bumpiness/severity. These results highlight the importance of accurate turbulence modelling in ensuring aircraft safety and assessing structural fatigue.

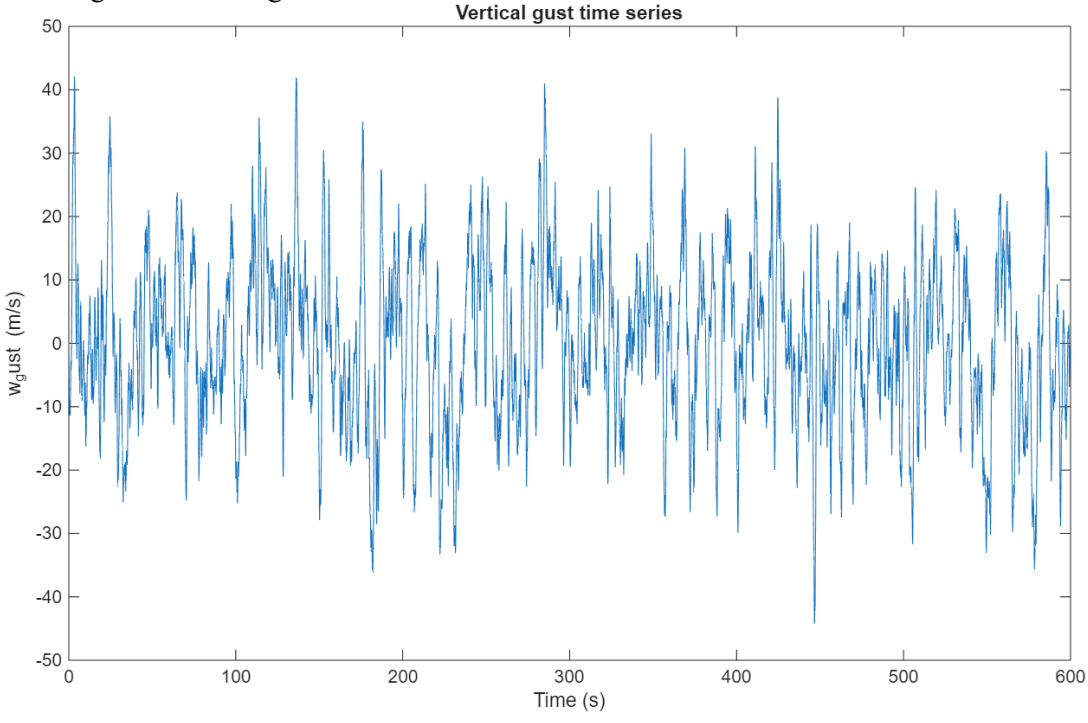

Fig. 1 Time-series of vertical gust velocity

- We similarly generate lateral and longitudinal gust components and compute their PSDs.
- The gusts generated above enter the aircraft dynamic equations through additive wind-velocity components in the body axes.
- We compute vertical acceleration, load factor – n_z – roll and pitch rates due to the gusts, and structural bending moments at wing root.

- The simulation uses a linearized flight dynamics model with added gust input.
- We next compute the load factor – n_z – wing-root bending moment based on acceleration and mass distribution.
- We also compute roll and pitch rate responses assuming lateral gust and attack-angle perturbation.

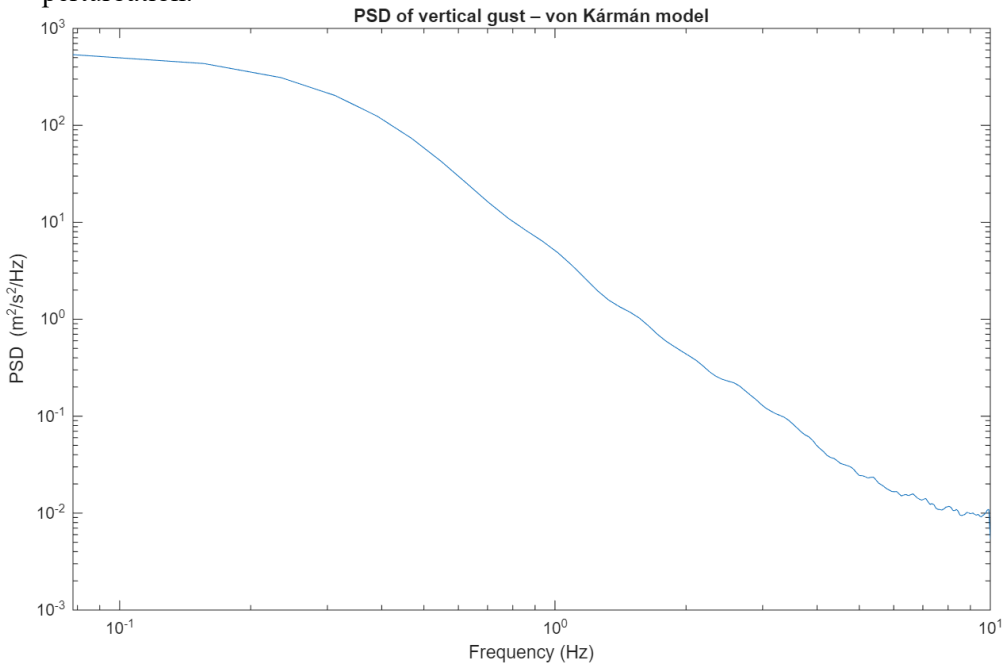

Fig. 2 PSD of vertical gust with von Kármán mathematical model

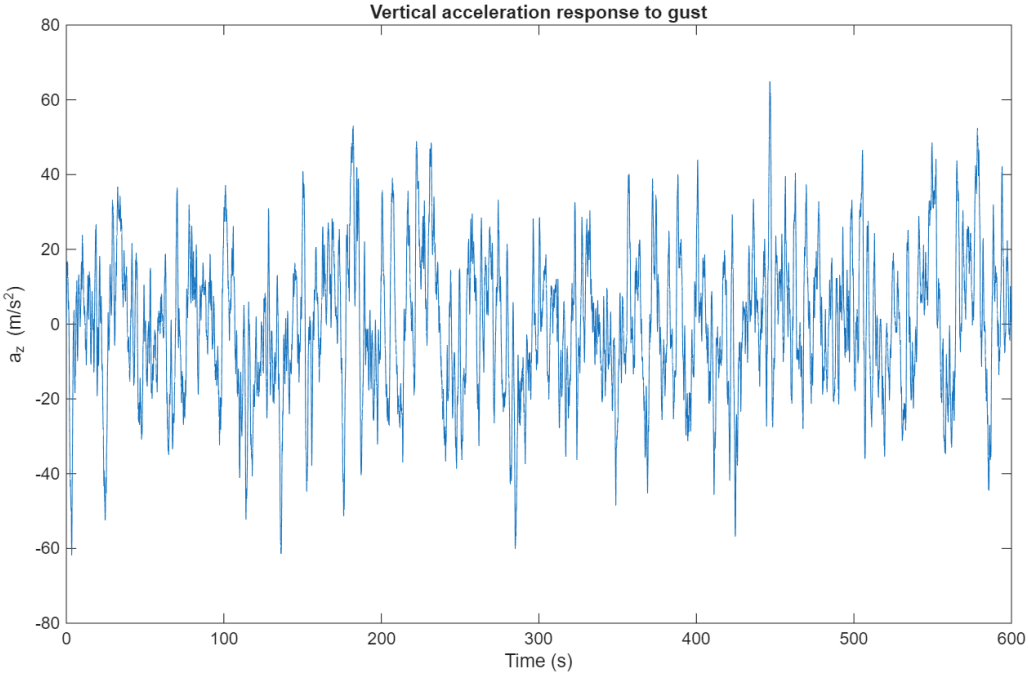

Fig. 3 Vertical acceleration response to gust

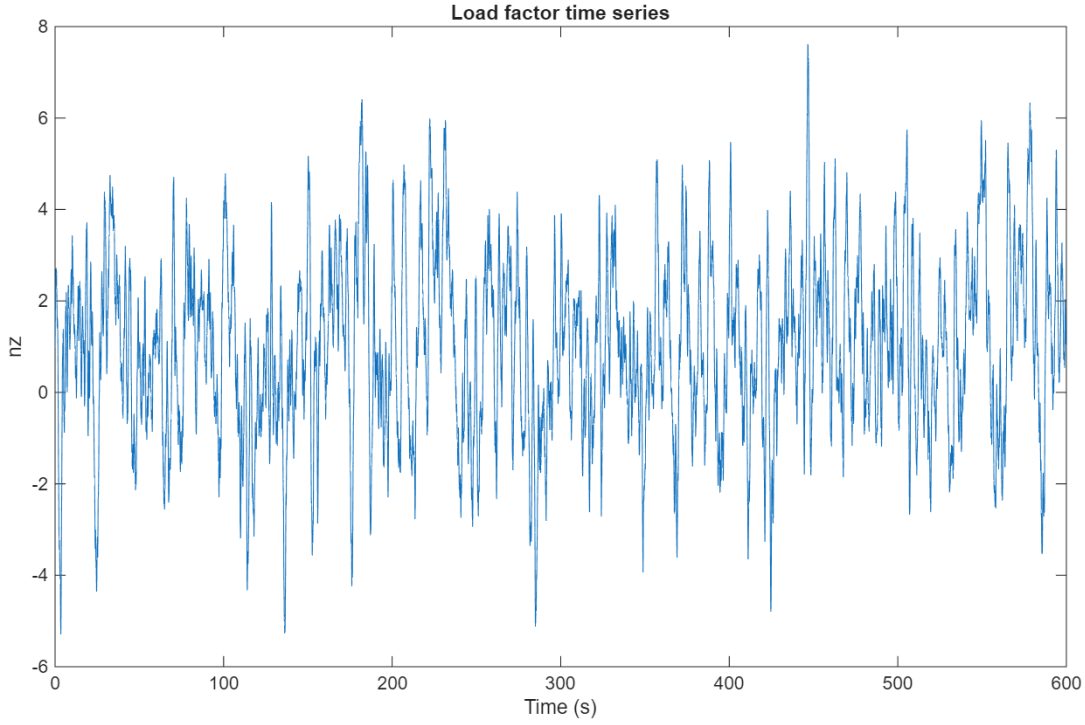

Fig. 4 Time-series of load factor

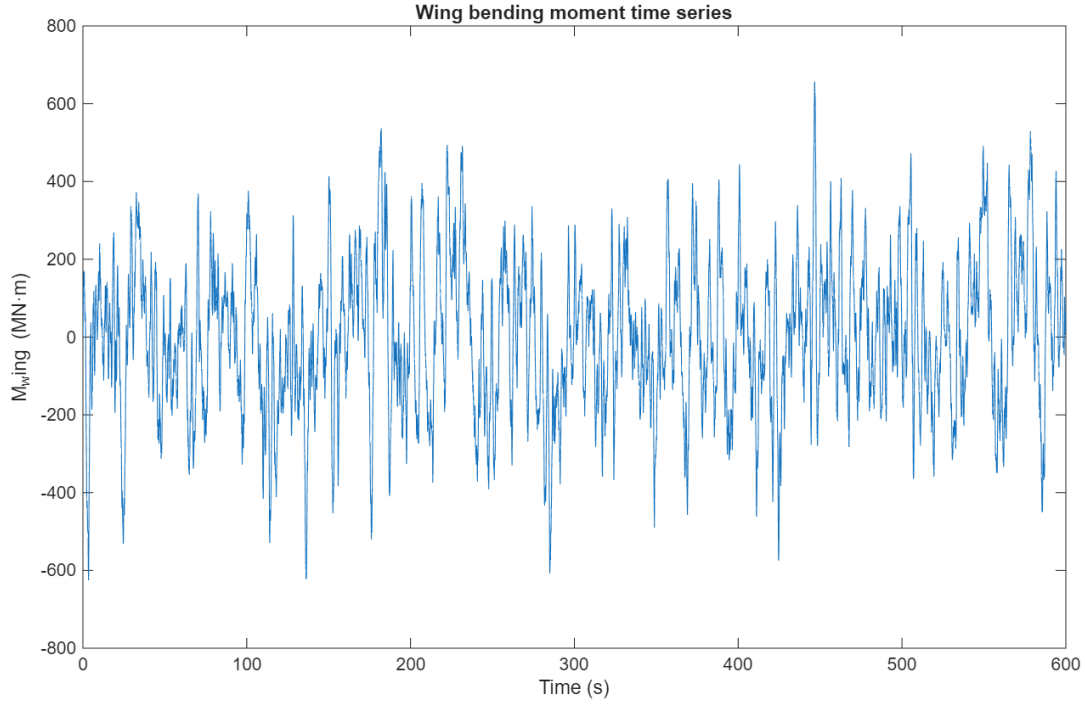

Fig. 5 Time-series of wing bending moment

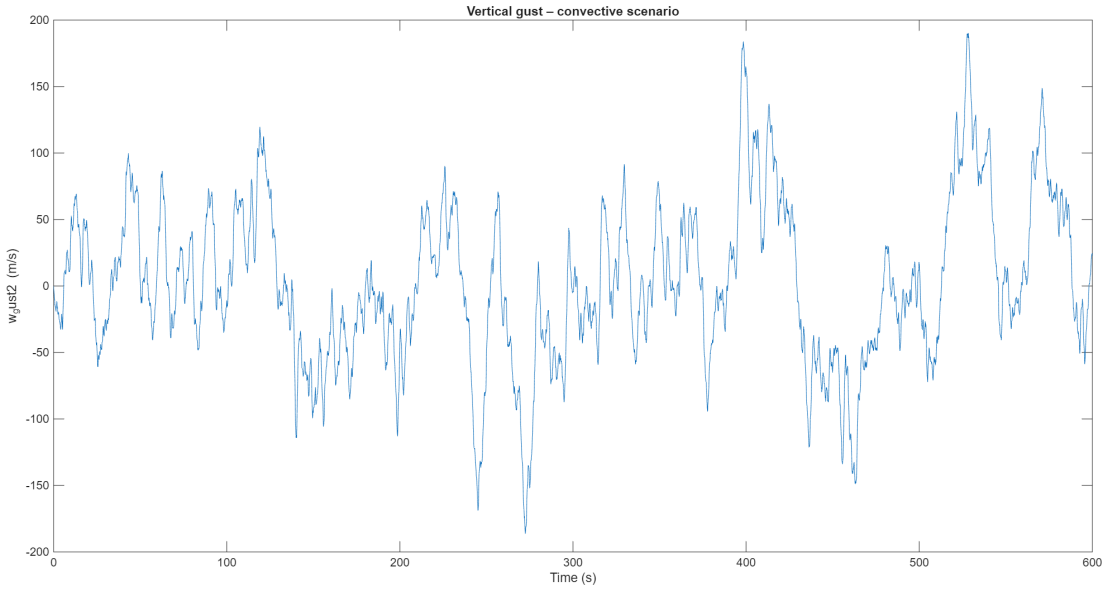

Fig. 6 Vertical gust – convective scenario

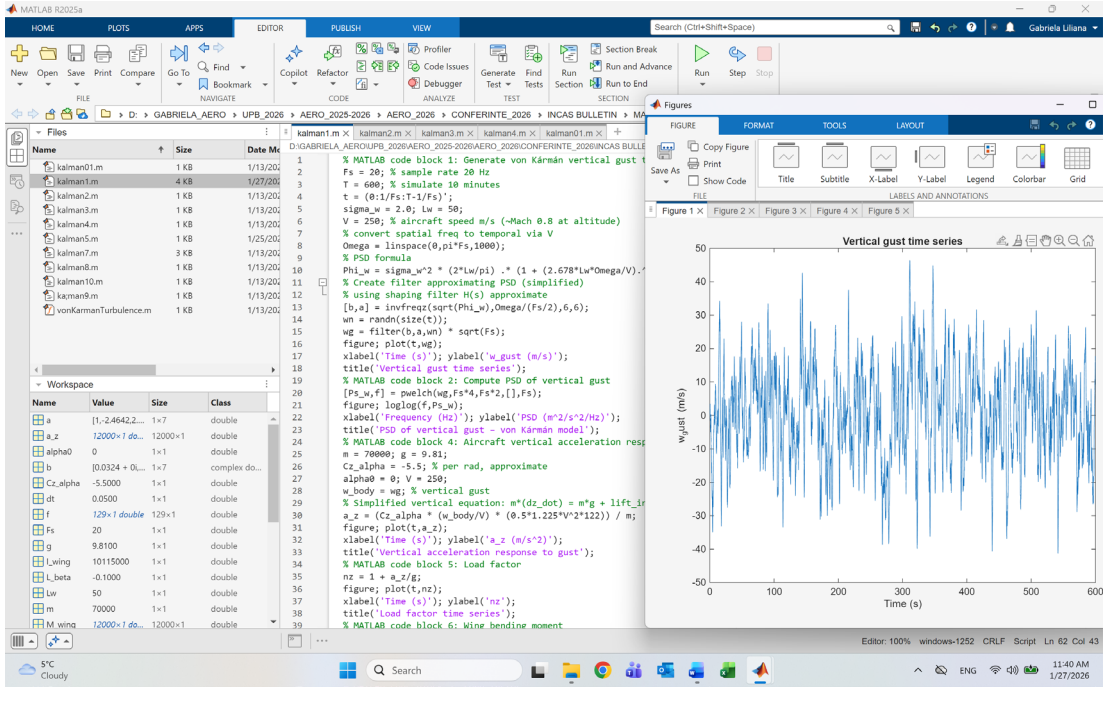

Fig. 7 Time-series of vertical gust velocity

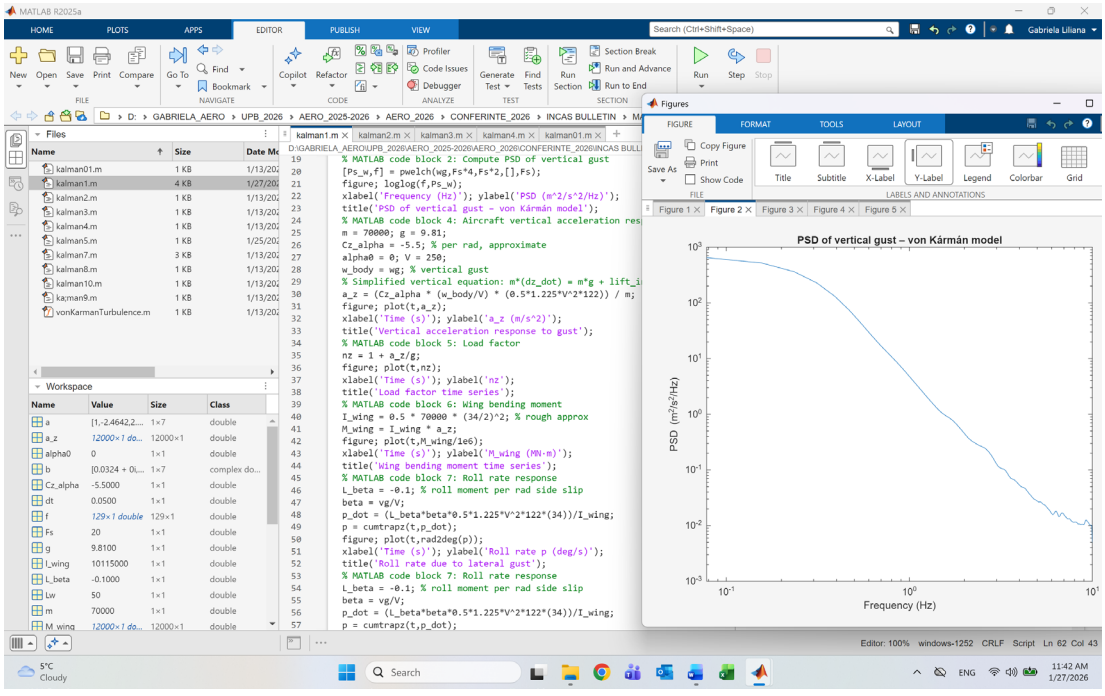

Fig. 8 PSD of vertical gust with von Kármán model

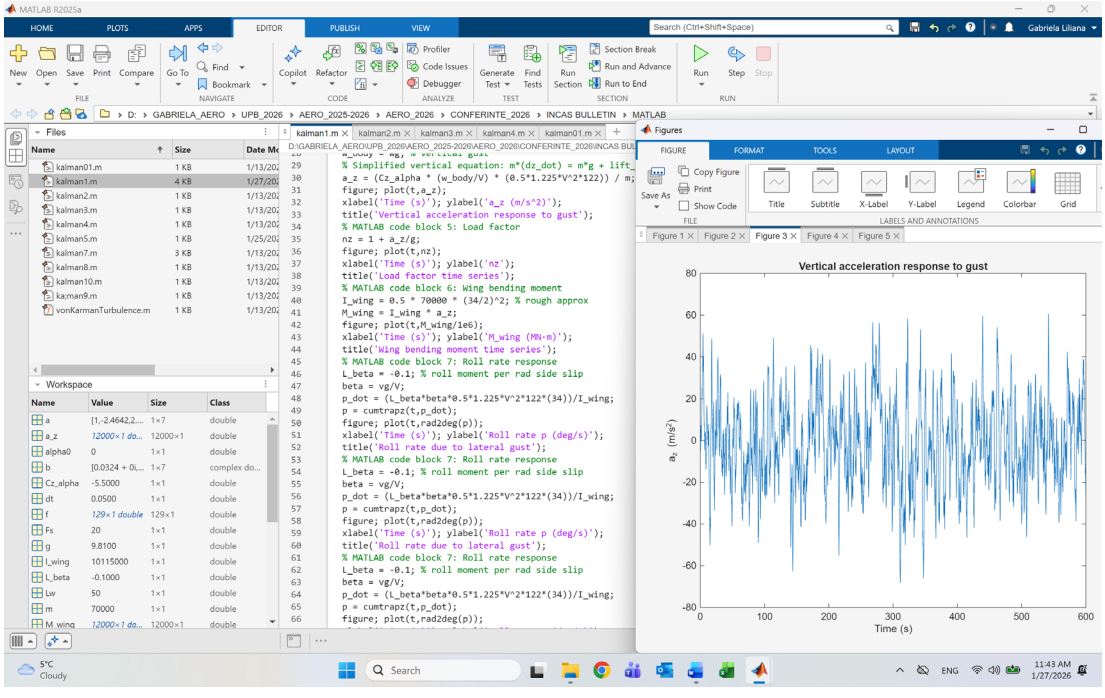

Fig. 9 Vertical acceleration response to gust

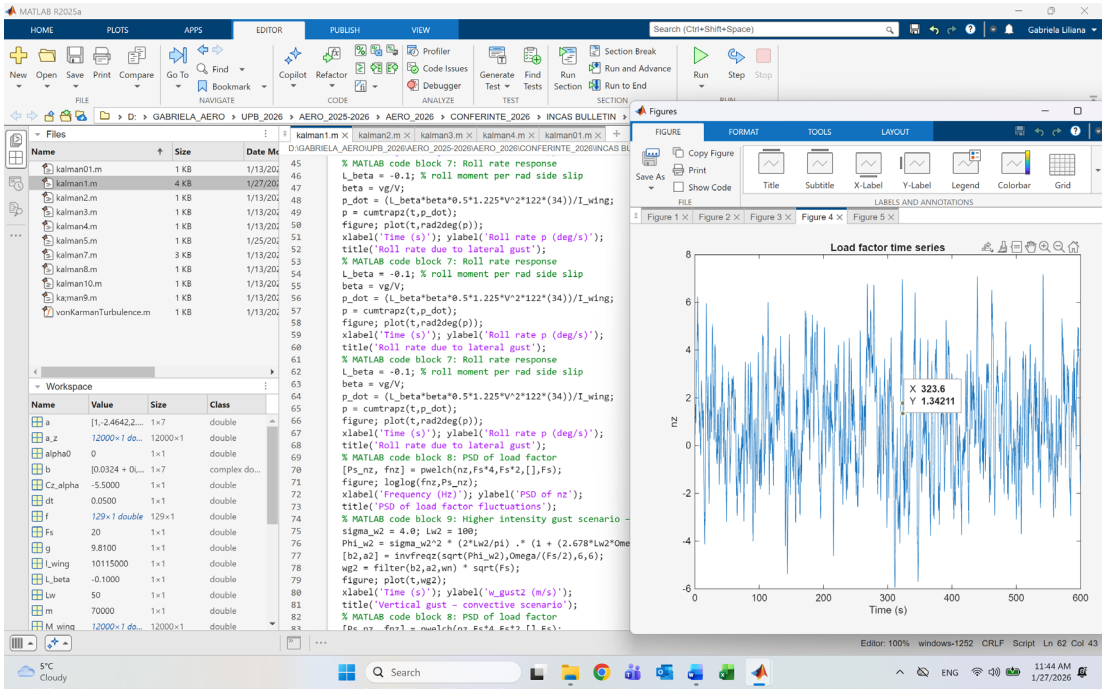

Fig. 10 Time-series of load factor

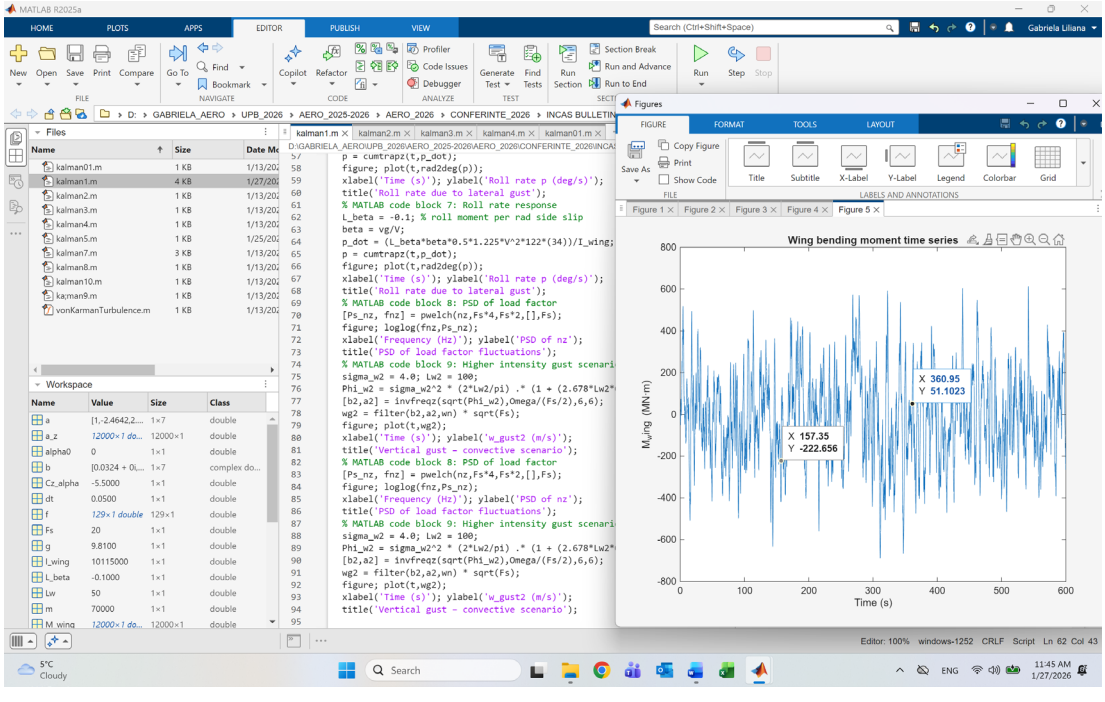

Fig. 11 Time-series of wing bending moment

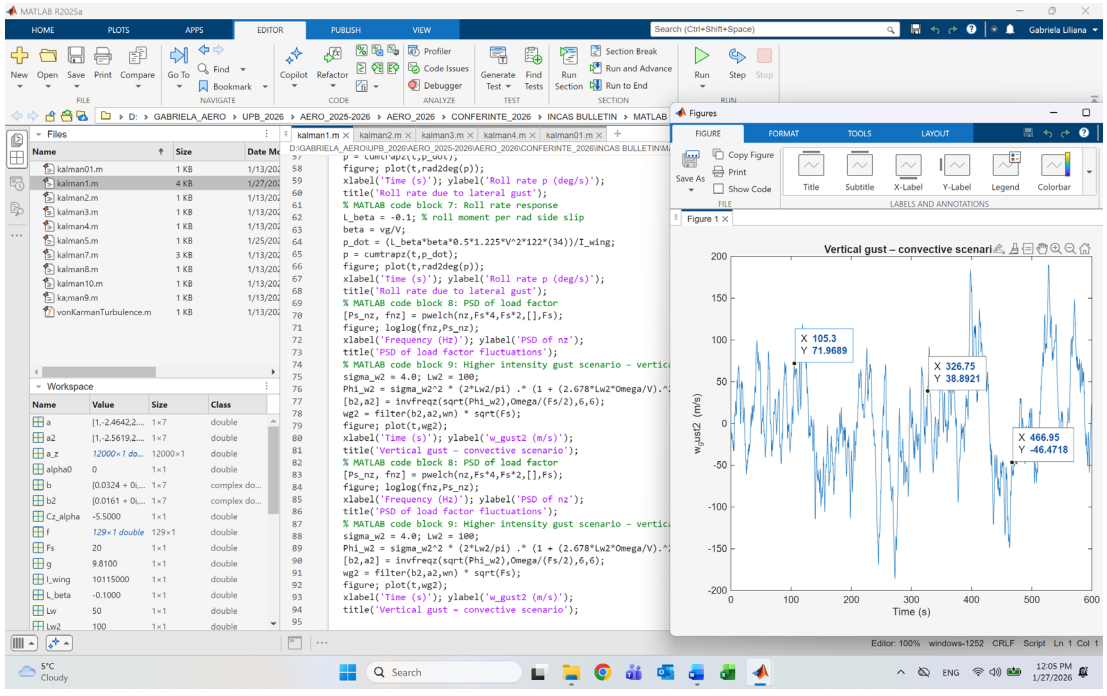

Fig. 12 Vertical gust – convective scenario

This study investigates the response of a commercial airliner cruising at high altitude over the Pacific Ocean through a region of intense convective activity, which results in strong turbulence. A stochastic gust field is generated using the von Kármán spectral model for continuous gusts, and the aircraft dynamics are simulated in MATLAB to evaluate acceleration, load factors, structural bending moments, and trajectory perturbations. Key results include time-series of gust wind components, power spectral densities, aircraft responses – including vertical acceleration and roll/pitch rates – and statistical metrics of bumpiness/severity. These results highlight the importance of accurate turbulence modelling for aircraft safety and structural fatigue assessment.

We assume that the aircraft is cruising at FL350 over the Pacific Ocean when it encounters a convective thunderstorm cell generating strong vertical motions, including updrafts, downdrafts, and enhanced turbulence. While detailed synoptic data are not available for this specific flight, convective turbulence adjacent to deep convective clouds has been documented.

In such an environment, turbulence intensities (σ) and length scales (L) may increase significantly. We adjust our gust model accordingly: $\sigma_w = 4$ m/s, $L_w = 100$ m for vertical component; $\sigma_v = 5$ m/s, $L_v = 120$ m for lateral component. We re-run the simulations, generate time-series and spectra and compare to the baseline case.

This study demonstrates how the von Kármán turbulence model can be used to simulate turbulence encounters for a civil aircraft over oceanic regions, how flight level and speed influence turbulence encounters and aircraft responses, and how it can provide a methodology for further investigation.

Key findings:

- Higher flight speed increases gust encounter frequency and may exacerbate aircraft responses.
- Turbulence intensity and scale length play major roles in determining response magnitude.

- Model assumptions must be treated carefully when applying to convective and oceanic environments.

Future work:

- Incorporate real meteorological datasets – e.g., from oceanic convective zones.
- Couple aircraft control/structural/elastic dynamics.
- Perform Monte Carlo simulations.
- Include in-flight measurement validation, if available.
- Extend the methodology to route planning or operational optimization.

REFERENCES

[1] * * * ATPL – Meteorology, CAE Oxford, 2020.
[2] J. R. Holton and G. J. Hakim, *An Introduction to Dynamic Meteorology*, Fifth Edition, 2013.
[3] D. McLean, *Automatic Flight Control System*, Prentice Hall International, 66 Wood Lane End, Hemel Hempstead, Herts HP2 4RG, 1990.
[4] B. L. Stevens and F. L. Lewis, *Aircraft Control and Simulation*, John Wiley, USA, 1992.
[5] * * * MATLAB Tutorials, 2025.
[6] * * * http://www.MathWorks, Inc. Aerospace Blockset, 2025.
[7] M. Rauw, *FDC 1.2. - A SIMULINK Toolbox for Flight Dynamics and Control Analysis*, May 10, 2001.
[8] D. Sheu, and Chuan-Tau Lan, Estimation of Turbulent Vertical Velocity from Nonlinear Simulations of Aircraft Response, *Journal of Aircraft*, Vol. **48**, No. 2, March-April, 2011, https://doi.org/10.2514/1.C031190.
[9] * * * https://ntrs.nasa.gov/api/20240003091/downloads/2023-RTE-Report_FINAL.pdf
[10] * * * https://rotorcraft.arc.nasa.gov/Publications/files/1682_Conley_Final_012324.pdf
[11] * * * https://ntrs.nasa.gov/api/citations/20070023367/downloads/20070023367.pdf
[12] * * * https://www.faa.gov/sites/faa.gov/files/pilots/pilot_handbook.pdf
[13]***https://home.engineering.iastate.edu/~shermanp/AERE355/lectures/Flight_Stability_and_Automatic_Control_N.pdf
[14] * * * https://iopscience.iop.org/article/10.1088/1742-6596/1005/1/012017/pdf
[15] * * * https://ntrs.nasa.gov/api/citations/20070023367/downloads/20070023367.pdf
[16] * * * https://d-nb.info/1254918787/34
[17] * * * ntrs.nasa.gov/api/citations/20240002719/downloads/AAMToolsForWildfire_FINAL.pdf
[18]* * * https://airbornescience.nasa.gov/sites/default/files/P-3B%20Experimenter%20Handbook%20548-HDBK-0001.pdf
[19] * * * https://iopscience.iop.org/article/10.1088/1742-6596/1005/1/012017/pdf